

## **Effect of Polarization Charges and Trapping Centres on Electron Transport Properties of $\text{Al}_{0.2}\text{Ga}_{0.8}\text{N}/\text{GaN}$ HFETs**

**H. Arabshahi**

*Department of Physics,  
Tarbiat Moallem university, Sabzevar, Iran  
Email: [hadi.arabshahi@sttu.ac.ir](mailto:hadi.arabshahi@sttu.ac.ir)*

### **Abstract**

Self-consistent Monte Carlo simulation has been developed and used to model electron transport in wurtzite phase AlGaN/GaN heterojunction FETs. Planer  $\text{Al}_{0.2}\text{Ga}_{0.8}\text{N}/\text{GaN}$  HFET structures with a 78 nm  $\text{Al}_{0.2}\text{Ga}_{0.8}\text{N}$  pseudomorphically strained layer were simulated, where the spontaneous and piezoelectric polarization effects were taken into account. The polarization effects was shown to not only increase the current density, but also improve the electron transport in the interface layer by inducing a higher electron density to the positive polarized sheet and away from the buffer layer.

### **Introduction**

Wide band gap GaN and related compounds with aluminium and indium currently have two main uses in commercial devices, providing bright LEDs emitting at ultraviolet-blue green wavelengths for CD-ROM and sensor applications and heterojunction field effect transistors (HFETs) which can sustain high current densities at elevated temperatures [1-2]. Further contributing to the outstanding performance of AlGaN/GaN based HFETs is the ability to achieve two dimensional electron gases (2DEGs) with sheet carrier concentration up to  $10^{13} \text{ cm}^{-2}$  close to the interface, well in excess of those observed in other III-V material systems. This is because of a lattice mismatch between AlGaN and its GaN buffer layer. In a typical AlGaN/GaN heterostructure an AlGaN layer is grown on top of a thick GaN layer. Because the lattice constant of GaN is larger than that of AlN (by about %2.5), the AlGaN is grown pseudomorphically, with a biaxial tensile strain and a compressive strain along its hexagonal *c*-axis [3,4]. This strain produces a macroscopic

piezoelectric polarization field in the AlGa<sub>0.8</sub>N interface. The direction of the field depends on the polarity of the AlGa<sub>0.8</sub>N growth surface. Recent studies have indicated that in typical AlGa<sub>0.8</sub>N/GaN, which are grown by metalorganic vapor phase epitaxy (MOVPE), this surface (which is [0001]) has cation polarity so that the orientation of the field is in the same direction as the growth [5]. This paper presents the results of two dimensional Monte Carlo simulation of electron transport in the wurtzite phase Al<sub>0.2</sub>Ga<sub>0.8</sub>N/GaN heterojunction FETs including polarization effects at room temperature. The simulations have been carried out using a non-parabolic ellipsoidal valley model to describe transport in the conduction band. This article is organised as follows.

Details of the device fabrication and polarization model which is used in the simulated device are presented in section II, and results for simulation carried out on Al<sub>0.2</sub>Ga<sub>0.8</sub>N/GaN heterostructure are interpreted in section III.

## Device, Model and Simulations

Figure 1 shows the structure of the simulated HFET which is based on the transistor studied experimentally and reported by Khan *et al* [6]. The device consists of a 78 nm top Al<sub>0.2</sub>Ga<sub>0.8</sub>N layer with doping density of  $5 \times 10^{23} \text{ m}^{-3}$ . An electron concentration of  $3 \times 10^{24} \text{ m}^{-3}$  is assumed for the source and drain contact regions. The overall device length is 3.5  $\mu\text{m}$  in the x-direction and the device has a 0.45  $\mu\text{m}$  gate length and 0.5  $\mu\text{m}$  source and drain length. The top and bottom buffer layers are doped to  $10^{23} \text{ m}^{-3}$  and  $10^{22} \text{ m}^{-3}$ , respectively. The effective source to gate and gate to drain separation are 0.8  $\mu\text{m}$  and 1.25  $\mu\text{m}$ , respectively. A Schottky barrier height of 1 eV for the gate electrode has been used to represent the contact potential at the Au/Pt. The source and drain have ohmic contacts which are modelled with the geometry shown in figure 1. The side contacts are intended to represent the remainder of the ohmic pads in the real device.

The ensemble Monte Carlo method used as the basis for this work was developed in Durham university and has been used extensively in the study of the electronic properties of many semiconductors and device structures including AlGaInP/GaAs HBTs, InGaAs/InP HEMTs and InGaAsP quantum well lasers [7-9].

In the case of the ellipsoidal, non-parabolic conduction valley model, the usual Herring-Vogt transformation matrices are used to map carrier momenta into spherical valleys when particles are drifted or scattered. The Monte Carlo simulation includes impurity scattering and all of the standard phonon scattering processes. It also allows for alloy scattering and piezoelectric scattering. The familiar five-valley approximation of the first two conduction bands has been used for the wurtzite crystal structure of GaN. In order to minimize the statistical fluctuations, always associated with the stochastic Monte Carlo method, we choose 20000 electrons with a Dirichlet boundary conditions for each mesh point. The timestep between two updates of the electric field is taken to be 1 fs.

Figure 2 illustrates the instantaneous distribution of 20000 electron particles at steady-state forward bias (drain voltage 30 V and gate voltage -1 V) superimposed on

the field cell mesh in the simulated HFET structure. In order to represent the polarization across the heterostructure interface, fixed superparticles (charge per unit length) are placed in the upper and lower of that layer as shown in figure 2, with the positive charge at the interface layer.

In the simulation presented here it is assumed that polarization charges are of density  $2 \times 10^{13} \text{ cm}^{-2}$  to take into account the spontaneous and piezoelectric polarization effects [10,11]. However, the positive polarization charge at the AlGaN/GaN interface tends to be compensated by the free electrons which are attracted to it. Because of the buffer layer's important role in high-field trapping effects, it is assumed in the simulations that trap centres are in buffer layer with density of  $10^{23} \text{ m}^{-3}$ , capture cross-section of  $2 \times 10^{-19} \text{ m}^2$  and energy of 0.3 eV. This trap centres are fixed at the centre of each electric field cell and captured some mobile charges.

## Results

To study the polarization effect on device performance, we have simulated the GaN HFET shown in figure 1 with and without the inclusion of the polarization effect. The simulation results indicate that the steady-state drift velocity and electronic transport properties of the device increase with the inclusion of the polarization effect across the interface which is in good agreement with the recent theoretical work done by Ando *et al.* [12] who were used two dimensional self-consistent full band Monte Carlo simulation for  $\text{Al}_{0.2}\text{Ga}_{0.8}\text{N}/\text{GaN}$  HFETs including piezoelectric polarization effects. The main reason for this can be understand from the simulated  $I$ - $V$  characteristic for the polarization and the polarization-free device, it can be observed that polarization leads to an enhancement of the drain saturation current from  $1250 \text{ mA mm}^{-1}$  to  $1650 \text{ mA mm}^{-1}$  at zero gate bias. This pattern of output current enhancement is due to the use of a heterostructure and the fact that the polarization charge encourages a higher electron density at the heterointerface where trapping does not occur and the electron mobility is high. The associated intrinsic transconductance derived from the current-voltage characteristics at knee voltage ( $\sim 18 \text{ V}$ ) for the simulated device without polarization charge and with including polarization charge are  $85$  and  $110 \text{ mS mm}^{-1}$ , respectively.

Figure 3 compares the electron density recorded from the buffer to the gate for both polarization and polarization-free devices. It can be seen that for the same bias condition the electron density in the interface region is increased for polarization device. This results an increase in electric field transverse to the channel and cause an enhancement in output drain current. Furthermore, high electric field in the gate and interface region can substain high velocities in these regions. We can estimate the speed of the device from the average electron transit time along the channel. By summary the transit times for each field cell we estimate the transit time to be  $\tau = 2.6$  ps. Hence the intrinsic cut-off frequency is about  $f_i = 1/2\pi\tau \approx 60 \text{ GHz}$ .

Figures 4a and 4b show a contour plot of the conduction band edge for the polarization and polarization-free devices, respectively. The source is located on the

left and the drain is on the right. It is noticeable that much of the drain-source bias in the polarization-free device is dropped in the vicinity of the gate region. The sharp drop in potential at the drain edge of the gate generates hot electrons which can diffuse into the AlGaN layer and also into the GaN buffer layer where they can be trapped.

In comparison figure 4b shows results for polarization charge density of  $2 \times 10^{13} \text{ m}^{-2}$ . It is seen that the presence of polarization charge reduces the sharp potential drop seen in figure 4a as a result of the high electron density around the heterointerface, and also strongly affects the potential between source and gate. This improves electron confinement, which is the main reason for a higher output drain current.

To study the effect of the magnitude of the polarization charge density on electronic transport in more detail, Monte Carlo simulations of steady-state condition were performed for a range of different densities. Figure 5a and 5b compare semiquantitatively the electron distribution around the heterointerface for two different charge densities. It can be seen that with increasing polarization charge density the number of electrons occupying the channel region increases. It can be calculated that the electron drift velocity increases from  $1.9 \times 10^5$  to  $2.7 \times 10^5 \text{ ms}^{-1}$  as  $\sigma$  goes from  $10^{12}$  to  $2 \times 10^{13} \text{ m}^{-2}$  due to an increased electric field transverse to the channel.

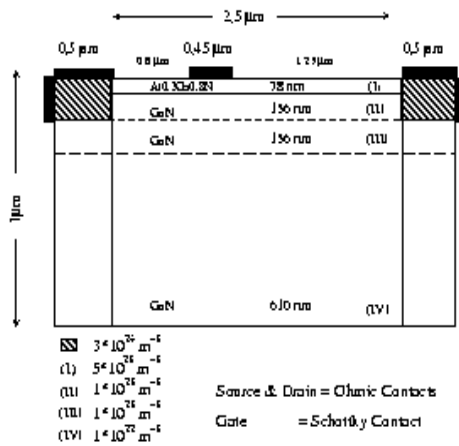


**Figure 1:** Cross section of the  $\text{Al}_{0.2}\text{Ga}_{0.8}\text{N}/\text{GaN}$  structures which have chosen in the simulation.

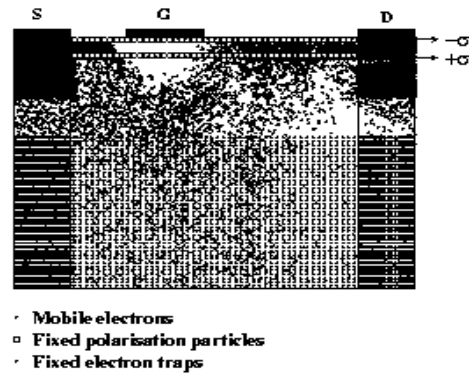


**Figure 2:** Particles in the Monte Carlo simulation of  $\text{Al}_{0.2}\text{Ga}_{0.8}\text{N}/\text{GaN}$  HFET are of two types. These are fixed particles which represent the polarization charges and trap centres and the mobile superparticles which represent unbound electrons which can flow through the device.

### Summary

In this article, we have presented the results of a Monte Carlo simulation for electron transport in  $\text{Al}_{0.2}\text{Ga}_{0.8}\text{N}/\text{GaN}$  HFETs which was developed to show the spontaneous

and piezoelectric polarization effects. Using valley model to describe the electronic bandstructure, calculated drain currents was shown the polarization effect not only increase the output current, but also improve the electron transport in the interface layer by inducing a higher electron density to the positive sheet and hence it can improve transconductance. The presented results are in fair agreement with other calculation. However, the simulation results can provide some guide to the range within which AlGaIn/GaN HFET with a specific polarization charge is expected to have the better performance.

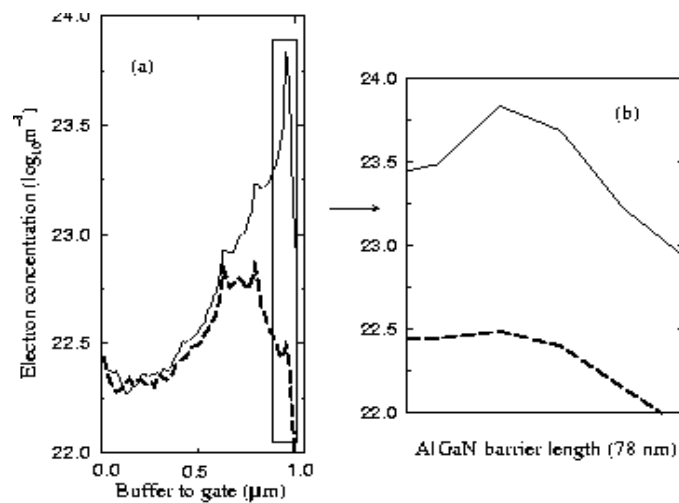


**Figure 3:** Electron density through the device under the gate extracted along the vertical line from the buffer to the centre of gate.

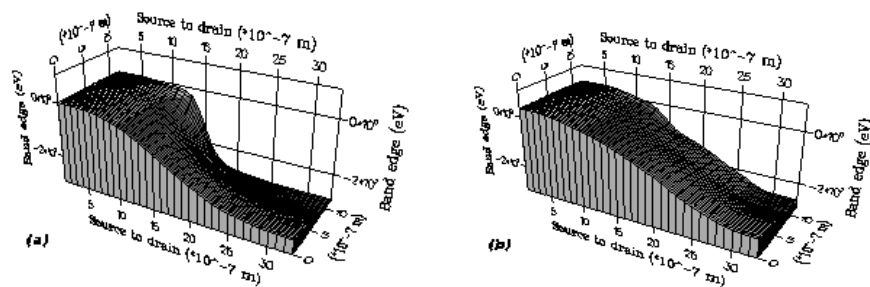


**Figure 4:** Three-dimensional distribution of the conduction band profile in the simulated GaN HFET at room temperature. (a) without polarization charge at the interface layer and (b) with polarization charge density.

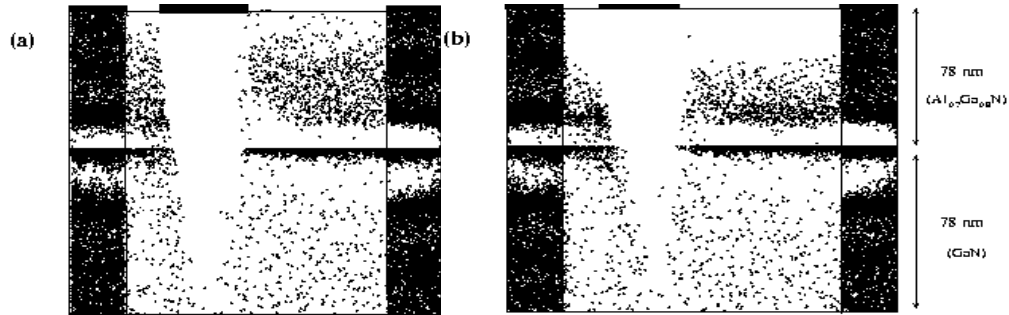


**Figure 5:** Effect of different polarization sheet charge densities on electron distribution through the wurtzite GaN HFET at room temperature when  $V_{gs} = -1$  V and  $V_{ds} = 30$  V. (a)  $\sigma = 10^{12} \text{ cm}^{-2}$  and (b)  $\sigma = 2 \times 10^{13} \text{ cm}^{-2}$ .

## References

- [1] S Nakamura, M Senoh and T Mukai, *Appl. Phys. Lett.* **62**, 2390 (1993)
- [2] S Strite and H Morkoc, *J. Vac. Sci. Technol.* **B 10**, 1237 (1992)
- [3] L Hsu, W Walukiewicz, *Appl. Phys. Lett.* **74**, 2405 (1999)
- [4] E T Yu, G J Sullivan and P M Asbeck, *Appl. Phys. Lett.* **71**, 2794 (1997)
- [5] A R Smith, R M Feenstra, D W Greve, J Neugebauer and J E Northrup, *Phys. Rev. Lett.* **79**, 3934 (1997)
- [6] M A Khan, J W Yang, W Knap, E Frayssinet and X Hu, *Appl. Phys. Lett.* **76**, 3807 (2000).
- [7] M Walmsley and R A Abram, *COMPEL – The International Journal for Computational and Mathematical in Electrical and Electronic Engineering.* **15**, 31 (1996)
- [8] D Hoare and R A Abram, *J. Electronics* **83**, 429 (1997)
- [9] G C Crow and R A Abram, *IEEE J. Quant. Elec.* **33**, 1190 (1997)
- [10] Ambacher, J Smart, J R Shealy, N G Weimann, K Chu and M Murphy, *J. Appl. Phys.* **85**, 3222 (1999).
- [11] Ambacher, B Foutz, J Smart, J R Shealy, N G Weimann, K Chu and M Murphy, *J. Appl. Phys.* **87**, 334 (2000).
- [12] Y Ando, W Contrata, N Samoto, H Miyamoto, K Matsunaga and M Kuzuhara, *IEEE Transactions on Electron Devices.* **47**, 1965 (2000).